JPP Journal of Pharmacy and Pharmacology

JPP 2005, 57: 689–698

Received November 29, 2004
Accepted February 7, 2005
DOI 10.1211/0022357056109
ISSN 0022-3573

Interaction of water with different cellulose ethers: a Raman spectroscopy and environmental scanning electron microscopy study

P. M. Fechner, S. Wartewig, A. Kiesow, A. Heilmann, P. Kleinebudde, R. H. H. Neubert

Abstract

Different non-ionic cellulose ethers like methyl cellulose (MC), hydroxypropyl cellulose (HPC) and hydroxypropylmethyl cellulose (HPMC) were investigated. The characterization of the cellulose ethers was carried out by thermogravimetry and sorption/desorption isotherms. Differences in the properties of the cellulose ether films were described by time-dependent contact angle measurements. Changes in molecular structure of the raw materials, gels and films caused by water contact were studied using Raman spectroscopy. Differences between the substitution types and changes due to the gel or film formation were observed. An environmental scanning electron microscopy (ESEM) technique was used to distinguish the morphological behaviour of the cellulose ether films in contact with water. Based on in-situ ESEM experiments, the swelling and drying behaviour of the various stages of cellulose ether films (film–hydrated film–dried film) were quantified by using image analysis.

Institute of Pharmaceutics and Biopharmaceutics, Martin Luther University Halle-Wittenberg, W.-Langenbeck-Straße 4, 06120 Halle, Germany

P. M. Fechner, R. H. H. Neubert

Institute of Applied Dermatopharmacy, Martin Luther University Halle-Wittenberg, W.-Langenbeck-Straße 4, 06120 Halle, Germany

S. Wartewig, R. H. H. Neubert

Fraunhofer Institute for Mechanics of Materials, Heideallee 19, 06120 Halle, Germany

A. Kiesow, A. Heilmann

Institute of Pharmaceutics, Heinrich Heine University Düsseldorf, Universitätsstraße 1, 40225 Düsseldorf, Germany

P. Kleinebudde

Correspondence: P. M. Fechner, Institute of Pharmaceutics and Biopharmaceutics, Martin Luther University Halle-Wittenberg, W.-Langenbeck-Straße 4, 06120 Halle, Germany. E-mail: fechner@pharmazie.uni-halle.de

Acknowledgement and funding: The authors would like to thank the Deutsche Forschungsgemeinschaft (DFG) for the financial support (Ne 427/12-1 and He 2125/13-1), and Markus Thommes for the sorption and desorption measurements.

Introduction

Various types of polymers, such as the non-ionic cellulose ethers methyl cellulose (MC), hydroxypropyl cellulose (HPC) and hydroxypropylmethyl cellulose (HPMC), are used as hydrophilic matrices in controlled-release drug delivery systems, as soluble coating materials or as viscosity-increasing agents (Rowe et al 2003). These polymers are able to absorb water and, therefore, polymers form hydrophilic three-dimensional networks. Aqueous gels or hydrogels are classified into three groups according to their network structure: covalently bonded polymer networks, physically bonded polymer networks and well-ordered lamellar structures (Flory 1974; Ofner & Klech-Gelotte 2002).

Water absorbed to celluloses can be found in at least three states: tightly bound to anhydroglucose units, less tightly bound and as bulk water (Zografi & Kontny 1986; Achanta et al 2001). Investigations of Methocel cellulose ethers confirmed the presence of different states of water in gels (McCrystal et al 2002). The degree of substitution and the crystallinity have an important influence on physicochemical properties. A comparison of different types of HPC shows that cellulose ethers of greater crystallinity and smaller degrees of substitution bind the first external monolayer water more strongly. Besides, they have a smaller capacity to absorb water vapour and a greater capacity for internal absorption (Alvarez-Lorenzo et al 2000).

Several studies describe the complex behaviour of cellulose ethers in solid dosage forms. Alderman (1984) gives a general overview about the use of different cellulose ethers in hydrophilic matrices. Mitchell et al (1993a) relates the hydration properties of HPMC to its particle size. Nokhodchi et al (1996a, b) examines the properties of tablets compressed of HPMC dependent on their moisture content and shows that increasing moisture content results in a reduction in thickness and density and in an increase in tensile strength of the tablets. The influence of viscosity grade of different HPMCs dependent on compression speed and force has also been investigated (Nokhodchi et al 1996c). The swelling behaviour of HPMC-based matrix tablets was described using

scattered light intensity (Gao & Meury 1996). The swelling properties were influenced by the drugs included (Mitchell et al 1993b) and the presence of hydrophilic excipients (Parakh et al 2003). The diffusion of drugs through HPMC gels depends on the gel concentration and the release of drugs from matrices containing cellulose ethers depends on the drug content too (Mitchell et al 1993c). The water mobility inside the gel layer has been characterized by NMR imaging (Rajabi-Siahboomi et al 1996). The volume increase of pellets coated with a mixture of soluble HPMC and insoluble ethyl cellulose was stronger with a higher amount of HPMC in the membrane. The particle swelling is a result of the hydrostatic pressure due to water imbibition (Hjärtstam & Hjertberg 1998). Siepmann et al (1999) combined diffusion, swelling and dissolution mechanisms and developed a new model to predict the release kinetics of controlled drug delivery systems containing HPMC. Many authors use cellulose ethers in combination with drugs or other excipients. Cellulose ethers were compressed to tablets with a controlled drug release or used to coat pellets.

The objective of this study was to characterize various cellulose ethers without ingredients and to study their behaviour in the presence of water. Cellulose ethers in the form of powders, gels and films were investigated by Raman spectroscopy and ESEM to monitor the molecular and morphological changes and to obtain fundamental information about the swelling and shrinking properties. These investigations were supplemented by thermogravimetrical measurements and sorption/desorption isotherms to determine the water vapour absorption and time-dependent contact angle measurements to estimate the rate of water absorption of the cellulose ether films. The advantages of combining Raman spectroscopy and environmental scanning electron microscopy (ESEM) are described in the literature (Levin & Lewis 1990; Hopfe & Füting 1995; Tai & Tang 2001; Donald 2002; Stokes et al 2002, 2003; Fechner et al 2003). Raman spectroscopy is capable of discriminating differences at the molecular level similar to infrared spectroscopy. Therefore, it can be used to identify celluloses and their derivates (Goral & Zichy 1990; Langkilde & Svantesson 1995; Sekkal et al 1995). Furthermore, unlike infrared spectroscopy, Raman spectroscopy allows the measurement of samples in an aqueous environment. Raman spectroscopy can also be used to determine the substitution degree of non-ionic cellulose ethers as an alternative method to NMR and gas–liquid chromatography (Alvarez-Lorenzo et al 1999). Electron optical methods are meaningful and popular to visualize morphological observations. However, in-situ experiments in electron microscopy are not widespread in pharmaceutical research. The advantage of the ESEM technique is that the sample can be treated with water during the experiment. Jenkins & Donald (1997) applied ESEM for in-situ hydration experiments to examine the swelling behaviour of cellulose fibres. In contrast thereto, we produced and characterized films made by soluble cellulose ethers and accomplished in-situ ESEM experiments.

Materials and Methods

Materials

Various substituted cellulose types were investigated: MC, HPC and HPMC (described in Table 1). Metolose was provided by Shin-Etsu (Japan), Methocel by Colorcon (Germany) and Klucel by Hercules (Germany). These HPMCs differ in their substitution type and in their viscosity.

Demineralised water was used as liquid in all experiments.

Table 1 Cellulose ethers arranged by their special substitution part of methoxyl and hydroxypropoxyl groups in the cellulose molecules

Substitution type	Methoxyl content (%)	Hydroxypropoxyl content (%)	Trade name	Sample no.
MC	ca 30	—	Metolose SM-4000	M1
			Metolose SM-15	M2
HPMC Type 2906	27–30	4.5–7	Metolose 65 SH-400	HM3
			Metolose 65 SH-50	HM4
HPMC Type 2910	28–30	7–12	Metolose 60 SH-4000	HM5
			Metolose 60 SH-10000	HM6
			Methocel E5 LV Premium EP	HM7
			Methocel E3 LV Premium EP	HM8
HPMC Type 2208	19–24	4–12	Metolose 90 SH-4000	HM9
			Metolose 90 SH-15000	HM10
			Methocel K100 Premium LV EP White	HM11
			Methocel K4M Premium EP	HM12
			Methocel K15M Premium EP White	HM13
HPC	—	ca 65	Klucel MF	H14

Arbitrary sample numbers are attached to simplify following assignments.

Storage of cellulose ethers in defined relative humidity

The cellulose ethers were stored under 0, 11, 22, 32, 43, 57, 75 and 90% relative humidity at 20°C for 14 days. Saturated salt solutions (Stahl 1980) were used to create the relative humidities.

Thermogravimetry and sorption/desorption

Thermogravimetrical measurements (TG 209, Netzsch, Germany) were performed after storage of the cellulose ethers under 43% relative humidity for 14 days. The cellulose ethers were heated with a rate of $10°C\,min^{-1}$ up to 150°C and kept isothermal for 10 min and mass differences were measured. The sample mass was in the range 10–30 mg. Sorption and desorption isotherms were obtained between 0% and 90% relative humidity under equilibrium conditions of 0.1% mass difference per 60 min using the moisture sorption test system SPS11 (Projekt-Messtechnik, Germany). The mass differences were determined dependent on the ambient relative humidity.

Gel and film forming

An adequate amount of water at 70°C was added to the cellulose ether powder. All particles were dissolved in hot water and cooled with ice under continuous stirring until the solution became a transparent gel.

Gel concentrations of 2% (m/m) cellulose ether were used to produce films. These gels (75 g) were placed into a mould of 120 mm diameter with a Teflon bottom side. After 24 h, the films were dried at 40°C for 72 h. The upper-side film surfaces were examined in all experiments.

Gel concentrations of 10% (m/m) cellulose ether were used for Raman spectroscopy. The influence of the amount of water on the gel formation was investigated for the gels containing 5, 10, 15, 20 and 30% (m/m) cellulose ether.

FT-Raman spectroscopy

Raman spectra were recorded on a Bruker FT-Raman spectrometer RFS 100/S (Bruker Optics, Germany) using a diode pumped Nd:YAG laser at an operating wavelength of 1064 nm. The measurements were performed using the 180° angle scattering geometry with 400 scans and a laser power of 250 mW at the sample location. Gel and powder samples were filled into glass tubes, while the complete films were placed directly in front of a mirror. The interferograms were apodized with the Blackman-Harris 4-term function and Fourier-transformed to obtain spectra with a resolution of $4\,cm^{-1}$. Evaluation of the spectra was carried out using the Bruker OPUS software version 4.2 (Bruker Optics).

Additionally, cluster analysis, including calculation of the spectral distances, was performed using the OPUS package Cluster Analysis.

Contact angle measurements

To investigate the behaviour of water in contact with the cellulose film, surfaces changes of the contact angle of water drops were measured for 180 s using the contact angle measuring system G10 (Krüss, Germany) at 20°C ($n = 17–20$). Photographs of the water drop of about 1 mm size were taken every 5 s. The contact angle was determined using the drop shape analysis system G2 inclusive the software DSA 1.1 from Krüss. To minimize the evaporation of water, contact angle measurements were carried out in a saturated relative humidity.

Deposition of metallic thin film structure

The deposition of the metallic thin film structures was done by conventional metal evaporation of silver using a mask to obtain shapes with defined slits, which were used to measure the distance changes. The coating had a thickness of about 200 nm. The widths of the slits were 45–57 μm.

Electron microscopy

The in-situ ESEM experiments were performed using an environmental scanning electron microscope (ESEM E3; ElectroScan, MA) with a LaB_6 cathode and an acceleration voltage of 10–20 kV. The investigations were carried out on the cellulose ether films with a silver film pattern on their surface. The sample was held at a constant temperature of 4°C using a water-cooled Peltier stage. During evacuation, the sample was kept wet by using an additional water reservoir. The ambient humidity was measured by a dew point sensor. Specific settings of the ambient humidity were achieved by changing the pressure inside the microscope chamber.

Experiments were conducted as follows: a free standing film sample of $5\,mm \times 5\,mm$ area with a thickness of about 100 μm was placed in the microscope chamber and documented by ESEM micrographs; the sample was moisturized at 100% ambient humidity for 10 min, which resulted in water drops on the Peltier stage and changes in the surface structure due to the water contact were documented by ESEM micrographs; the sample was dried and structural alterations were again documented by ESEM.

Image analysis

The quantitative assessment of the process was done by applying the image analysis software analySIS 3.1 (Soft Imaging System GmbH, Germany). Three line profiles rectangular to the border between the silver slits and the cellulose ether film were analysed automatically with respect to the grey values. These profiles ($n = 3$) were used to determine the thickness of the uncoated layer.

Statistical analysis

The unpaired *t*-test and the one-way analysis of variance post-hoc test (Tukey's multiple comparison test) were

used for the determination of significant differences in this work (GraphPad Prism 03, biostatistics, curve fitting, and scientific graphing). $P < 0.05$ denoted significance in all cases.

Results and Discussion

Water vapour absorption

Sorption and desorption isotherms characterize the water vapour absorption and desorption behaviour and were measured at constant temperature. Thermogravimetrical measurements were carried out to determine the water amount, which is absorbed by the substance or a part of its crystal structure. In contrary to the sorption/desorption measurements, thermogravimetry quantifies the water amount at constant humidity.

Sorption and desorption isotherms of M1 and H14 are depicted in Figure 1A. The cellulose ether types MC and HPMC showed similar sorption and desorption isotherms with hysteresis. However, the isotherms of HPC differ from those of the two other types, because sorption and desorption seem to be identical. Alvarez-Lorenzo et al (2000) observed a smaller hysteresis for HPCs than for low-substituted HPCs. It can be suggested that monolayer water is bound less strongly to HPCs and resulted in smaller differences between sorption and desorption than observed for the other cellulose ethers. The water vapour absorbed to the molecules in different kinds of binding. Stahl (1980) described the sorption process as connection of water bound to the molecule connected with stuffing of pores, which correlates with the different states of water, solid-like, bound and free, investigated in organic molecules described by Zografi & Kontny (1986).

Sorption/desorption and thermogravimetry differ significantly because the thermal energy transmitted due to heating up to 150°C results in a higher loss of bound water than for storage under phosphorus pentoxide. Nevertheless, both methods show that it is possible to classify the cellulose ethers according to their substitution level due to the amount of absorbed water vapour (Figure 1B). The analysis of variance test revealed significant differences ($P < 0.05$) between the cellulose ethers of the HPMC types 2906, 2910 and 2208. The highest water vapour absorption capacity was observed by HPMCs of the type 2208, for which the combination of low methoxyl and high hydroxypropoxyl content is characteristic (average methoxyl/hydroxypropoxyl substitution ratio 2.8). Substitution type 2910 showed the smallest water vapour absorption. This type is characterized by a high content of hydroxypropoxyl and methoxyl groups, which results in a higher average methoxyl/hydroxypropoxyl substitution ratio of 3.3. It can be assumed that the methoxyl content seems to be disturbing the process of water absorption; the methoxyl group is more lipophilic while the OH group in the hydroxypropyl substituent allows an interaction with water. In this context, Malamataris et al (1994) observed for various HPMCs that a decreasing moisture content correlated with increasing methoxyl/hydroxypropoxyl substitution ratio.

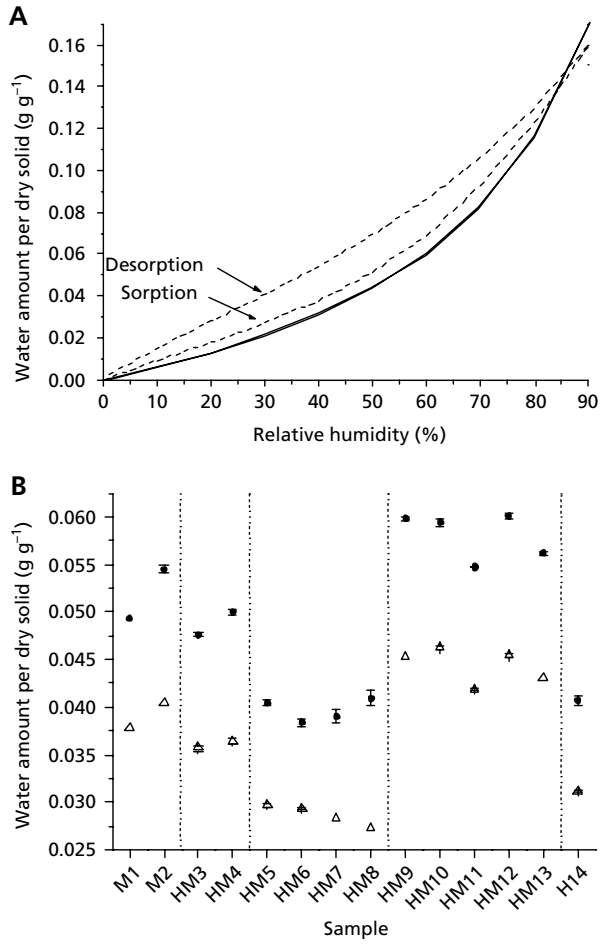

Figure 1 Water sorption behaviour of the cellulose ether types. A. Sorption and desorption isotherms of MC M1 (dashes) and HPC H14 (solid line). B. Water amount per dry solid using thermogravimetrical analysis (●; 43% r.h., n = 2 or 3) and weighing within the sorption process (△; 40% r.h., n = 1 or 2); maximum s.d. 0.0007 g water/g dry solid.

Raman spectroscopy

Comparison of raw materials

The Raman spectra of the raw materials: MC (M1), HPC (H14), and the three HPMCs (HM3, HM5 and HM9) are shown in Figure 2.

The Raman spectrum of cellulose shows several prominent vibrations (Table 2): namely, COC stretching modes, anhydroglucose ring vibrations, CO stretching modes and various modes of CH_2 deformation. Stretching modes of the CH, CH_2 and CH_3 groups (summarized as CH_x) are found between 2800 and 3000 cm^{-1} (Blackwell et al 1970; Edwards et al 1994, 1997).

Comparing the Raman spectra of cellulose ethers with those of each other and with that of cellulose, differences in the band positions and in the band intensities can be observed (marked with arrows, Figure 2) due to the different substituents, methoxyl and hydroxypropoxyl.

The Raman spectrum of the HPC H14 showed the strongest differences. Shifted band positions and higher

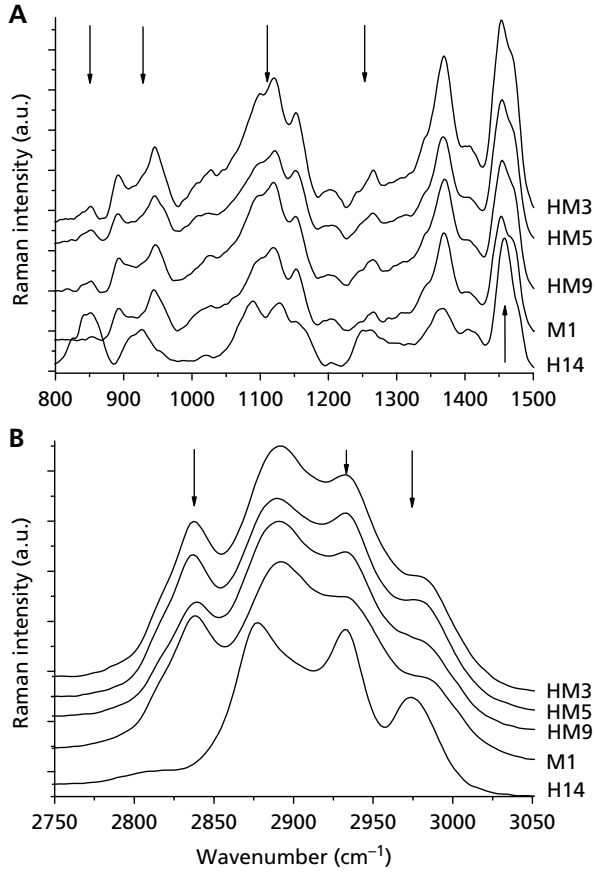

Figure 2 Raman spectra of the cellulose ether raw materials in the spectral ranges 800–1500 cm^{-1} (A) and 2750–3050 cm^{-1} (B); from bottom to top: H14, M1, HM9 (type 2208), HM5 (type 2910) and HM3 (type 2906). Differences are marked by arrows.

and lower band intensities were observed. In the range of the CH_x stretching modes three bands were visible, which are situated at 2877, 2933 and 2974 cm^{-1}. For MC M1, the spectral feature in the CH_x region shows a splitting into four bands at 2838, 2892, 2932 and 2982 cm^{-1}. The Raman spectra of HPMCs HM3, HM5 and HM9, which contain hydroxypropoxyl and methoxyl substituents, showed features of both substitution types of MC and HPC and each cellulose ether type exhibited a typical Raman band pattern.This was observable on the bands at about 852 cm^{-1} and in the range 1000–1200 cm^{-1}. A type-dependent splitting of the spectral features in the CH_x stretching range between 2800 and 3100 cm^{-1} is visible. An increase in the methoxyl content resulted in an increasing band intensity at about 2838 cm^{-1}; an increase in the hydroxypropoxyl content resulted in the increasing band intensities at about 2932 and 2974 cm^{-1}. Due to these changes in the band intensities in the CH_x range, a cluster analysis (Otto 1999) of the spectra allows differentiation of the HPMCs according to their types (Figure 3). Based on this procedure, the difference between HPC and MC/HPMCs is obvious (separation step A, Figure 3). H14 shows the highest heterogeneity mentioned above. In step B, HPMCs and MC are separated. Finally, the different HPMC substitution types are distinguishable (separation step C). Therefore, the cluster analysis allows the classification of cellulose ethers with regard to their substitution type, but it is not possible to discriminate the substances concerning their viscosity grade.

Previous spectroscopic studies of cellulose ethers assigned bands in the range 500–1500 cm^{-1} to the ether COC stretching vibration between 820 and 890 cm^{-1} and the CC stretch of alkyl side chains between 900 and 950 cm^{-1} (Langkilde & Svantesson 1995; Alvarez-Lorenzo

Table 2 Assignment of the most important Raman bands of cellulose and cellulose ethers according to literature data (Blackwell et al 1970; Edwards et al 1994, 1997; Langkilde & Svantesson 1995; Alvarez-Lorenzo et al 1999)

Assignment	Band positions (cm^{-1})		
	Cellulose	Cellulose ethers	
		MC	HPC
CCC ring deformation	333	—	—
	349		
	380		
CCO ring deformation	437	—	—
	460		
COC deformation of glycosidic linkage	496	—	—
	520		
ether COC stretching mode	—	893	852
	900	944	927
COC stretching mode of glycosidic linkage	1097	—	1090
	1122	1119	1129
Ring CC stretching mode	1153	1153	1151
CH_2 deformation	1380	1369	1367
	1470	1453	1458
CH stretching mode	2850–3000	2838	—
		2892	2877
		2932	2933
		2982	2974

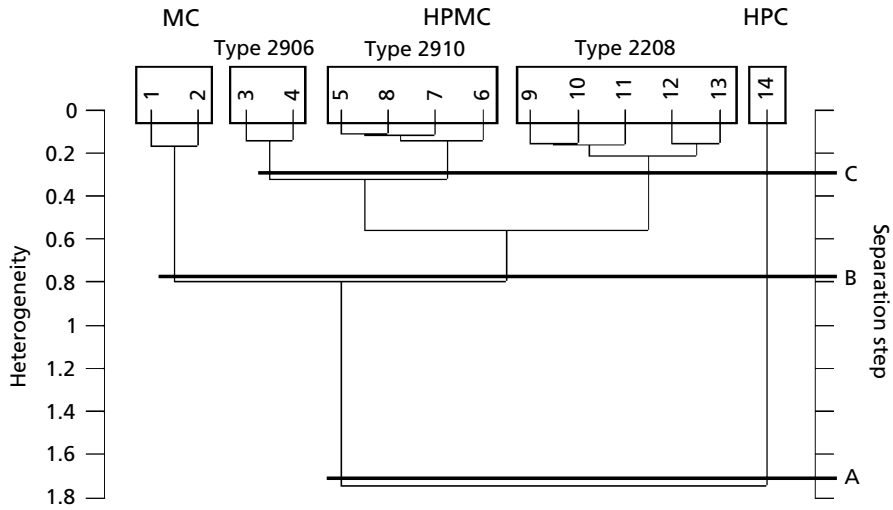

Figure 3 Cluster analysis of the Raman spectra of all cellulose ether raw materials; selected spectral range of 2800–3100 cm^{-1}. The spectra were pre-treated by the second derivative and vector normalization.

et al 1999). Alvarez-Lorenzo et al (1999) quantified the hydroxypropoxyl content using the bands of alkoxyl side chains at 1260 cm^{-1} (CC bonds) and at 1458 cm^{-1} (methyl/methylene region 1440–1475 cm^{-1}) in reference to the band at 1367 cm^{-1} belonging to CH bonds of the anhydroglucose skeleton. With regard to these investigations, the pattern in Raman spectra of HPMCs can be explained depending on their degree of substitution. Assuming normalization to the band at 1369 cm^{-1}, increasing hydroxypropoxyl content resulted in increasing band intensities at 852 cm^{-1} and at 1453 cm^{-1}.

Comparison of powder, gels and films

The Raman spectra of the raw materials and gels of M1 and H14 are depicted in Figure 4A. With the addition of water, the cellulose swells as a result of hydrogen bond formation. Due to the gel formation, changes in the entire Raman spectrum appear. The presence of water influences the CH_x stretching region between 2800 and 3100 cm^{-1} where the band positions and intensities change clearly. For the gel, the most intense band can be found at about 2940 cm^{-1}. Additionally, the intensity ratio of the bands of the COC glycosidic linkage at 1090 and 1120 cm^{-1} changed. When the content of cellulose ether decreased from 30 to 5%, only a decrease in the signal-to-noise ratio can be detected (Figure 4B). No further shift of the Raman bands was observed due to the increasing water amount. So it can be assumed that the cellulose ethers are fully hydrated in 30% gel formulations. Additionally, the influence of water vapour on Raman spectra of raw material of the cellulose ethers was investigated. Cellulose ether powders were measured after the storage at defined relative humidity between 0 and 90%. The resulting spectra show a shift of band positions in the CH_x stretching region dependent on the storage at a defined relative humidity (Figure 4C): with increasing relative humidity from 0 to 90%, a shift in band position from lower to higher wavenumbers occurred. The comparison of the Raman spectrum of the raw material M1 with that of the film is presented in Figure 4D. For the film, the same spectral features without shifts in band positions were observed as for the gels. The intensity ratios I_{1096}/I_{1120}, I_{2838}/I_{2890} and I_{2932}/I_{2890} can be served as measure for this behaviour. It could be evidence for the fixation of the network structure of the gels in the film. The addition of water to the cellulose ether films resulted in their gel spectra due to the gel-forming process.

Summarizing, the influence of water vapour on the raw material of the cellulose ethers in the Raman spectra was proved. Furthermore, the Raman spectra of the gels show clear differences in comparison with the raw material. For gels with a content of cellulose ether of 5–30%, the Raman spectra are almost identical. After drying the gels the changed molecular structure of the cellulose ethers remains. A correlation between morphological behaviour and molecular properties in their Raman spectra were shown.

Contact angle measurements on cellulose ether films

A water drop shows different behaviour on each solid surface. The contact angle is dependent on the energy of the surface, where the drop is placed and the surface structure, like chemical composition and roughness (Zografi & Johnson 1984; Palzer et al 2001). Wettability properties (wetting and spreading of liquids on surfaces) can be estimated by measuring the contact angles. The absorption of a water drop by cellulose ether film surfaces can be characterized by time-dependent measurements of the contact angle. The decrease of the water drop height is dependent on the rate of absorption and the amount of water evaporation. The experiment is based on behaviour of water drops

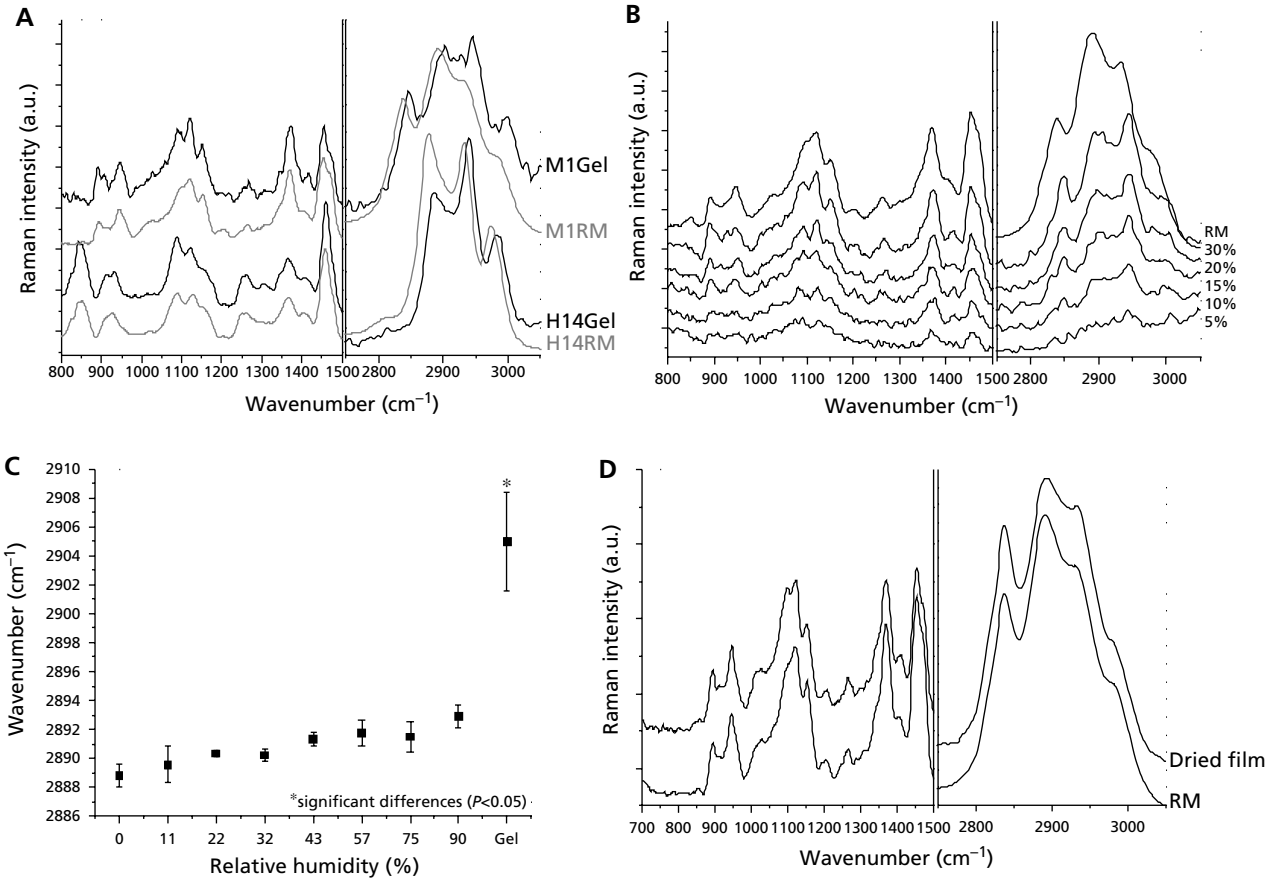

Figure 4 Results of Raman spectroscopy. A. Raman spectra of raw materials (RM) and gels of MC M1 and of HPC H14, respectively. B. Raman spectra of the HPMC HM9 of raw material (RM) and gels with different water content (spectra are not normalized). C. Shifts of one Raman band of the CHx stretching modes of cellulose ether raw materials due to storage in defined relative humidity (between 0% and 90%) compared with shift in band position of Raman spectra of cellulose ether gels (sample HM9; n = 4–9). D. Raman spectra of the MC M1: raw material (RM, bottom) and dried film (top).

on the surface of cellulose ether films, which swell due to the absorption of water into its network.

The contact angles of a water drop versus time are shown for all celluloses in Figure 5. Immediately, after setting the drop, a water contact angle of the cellulose ethers near 95° was measured, which is twice that measured by Sebti et al (2003). All measurements showed a declining curve, which can be fitted with a linear plot. All cellulose ethers showed the same rate of water drop absorption of $-0.14° s^{-1}$. However, two curves were separate from the others. HM5 showed a smaller contact angle, which could be a result of capillary effects. Following, the water could be partially sucked in the holes of the surface. This might explain the lower contact angle of HM5 as a result of the different surface structure. For H14, the curve can be divided into two parts. The first part of the curve exhibits a five times higher slope (rate of water drop absorption $-0.8° s^{-1}$), indicating that the water absorption was faster than in the second part, which was similar to the other celluloses. A similar behaviour of H14 was observed during the in-situ ESEM experiments, showing that the interaction with the water

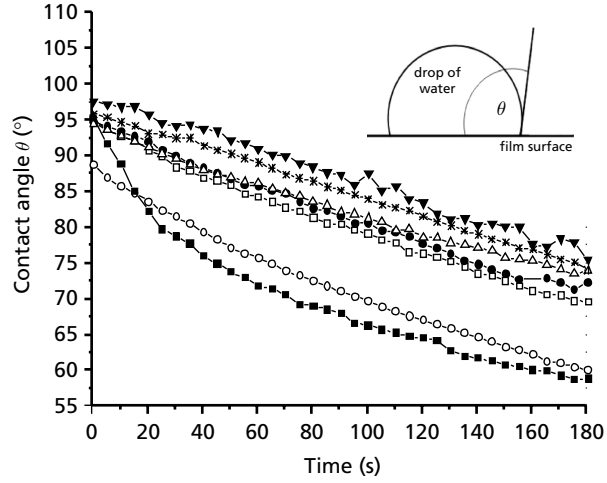

Figure 5 Contact angles of a water drop on cellulose ether films versus time (□, M1; ○, HM5*; ●, HM9; ▼, HM11; △, HM12; *, HM13; ■, H14*). The contact angle θ is the angle between a tangent of the drop surface and film surface (small picture); average of contact angles per time (n = 17–20) with relative s.d. between 5 and 17%; $*P < 0.05$.

drops was much faster than with the other cellulose ethers. The greater roughness of H14 might facilitate the faster imbibition of the water drop in the first part of water absorption, which could be connected with higher capillary effects. This also might be due to the more hydrophilic character of HPC. Despite the faster water absorption, the initial contact angle of H14 was comparable with that of the other cellulose ethers. In this connection, HM5 and H14 showed the lowest water vapour absorption capacity of the examined cellulose ethers.

In-situ ESEM experiments

The film surfaces of M1, HM9, HM12 and HM13 are more or less structured; H14 seems to have the roughest structured film surface. Unlike these, HM5 seems to have holes in the film surface and HM11 has small irregularities (wrinkles) on the surface.

Cellulose ether films swell when they are in direct contact with water. Therefore, it is of interest to characterize the swelling behaviour of such films, particularly with an optical method. A conductible coverage is not necessary for ESEM investigations; however, for this study, the films were covered with a pattern of thin silver slits to improve the contrast for electron microscopy and to give reference points for observation and monitoring.

ESEM micrographs of film surfaces at the end of the in-situ experiments, which show the silver layer left and right and the uncovered cellulose film midway, are depicted in Figure 6A–D. Changes in the structures of the thin silver film due to swelling and drying of cellulose ether and due to electron beam influence are visible: smaller and bigger wrinkles appear (Figure 6A, D) and rents in horizontal direction only in the thin silver film (Figure 6C). With HM11 (Figure 6B), rents also occurred within the uncoated layer and parallel to the border. This might indicate a different swelling behaviour of HM11 or different adhesion of the silver layer. Unfortunately, the contrast between the silver layer and the cellulose film was insufficient and, therefore, changes due to swelling could only be measured with less precision. During the experiment, M1 showed high electron beam sensitivity and further evaluation was not possible.

A method was developed to describe the behaviour of free cellulose ether films in contact with water and based on analysing ESEM images. The relatively plane film surface with small contrast causes difficulty in observing and measuring morphological changes. Therefore, a method to obtain quantitative information about the swelling/drying behaviour of the different films was needed. A thin metallic coating with specific structures (metallic thin film structures) was used to cover the surface to produce regions observable during the entire swelling/drying process. To evaluate swelling and shrinking quantitatively, the distance between two coated layers (i.e. the width or uncoated layer) was determined by image analysis. Figure 6E, F shows the grey scale values of HM12 and HM13 in original, swollen and dried state. The distance of the uncoated layer was set at 100% and the distances in

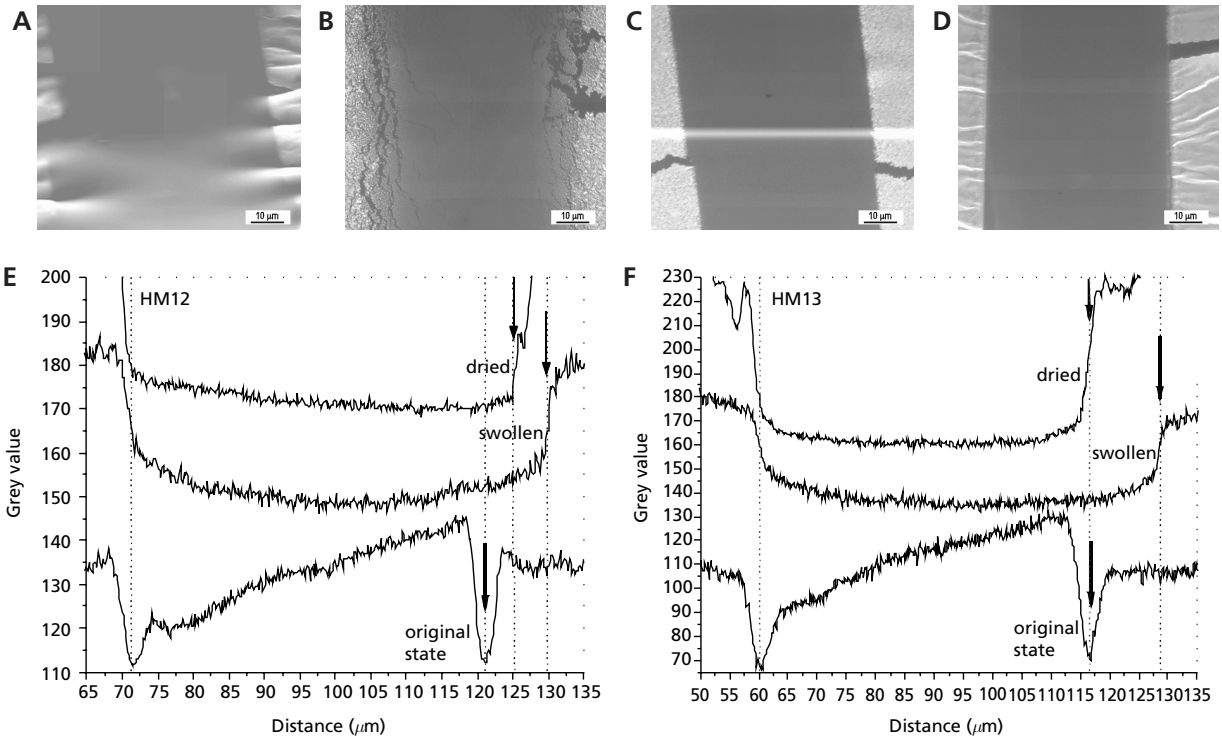

Figure 6 ESEM micrographs taken during the in-situ swelling experiment of the dried HPMC samples: HM9 (A), HM11 (B), HM12 (C), HM13 (D) (bar = 10 μm). Swelling behaviour of HM12 (E) and HM13 (F) analysed by image analysis program.

Table 3 Results of in-situ ESEM experiments: swollen and dried state of various cellulose ethers

Sample no.	Swollen state (%)	Dried state (%)
M1	n.d.	n.d.
HM5	112	106
HM9	114	120
HM11	113	118
HM12	118	108
HM13	120	100
H14	111	100

swollen or dried state were related to 100%. The swelling represented in Figure 6F is totally reversible, but in Figure 6E the swelling is only a partially reversible process. Noticeably, HM9 and HM11 showed an increase in distance after drying, which cannot be explained at the moment.

The results of swelling and subsequent drying are summarized in Table 3. All cellulose films swelled and showed an increased distance in the range 10–20%. HM5 and H14 showed the smallest capacity of water vapour absorption of all the examined cellulose ethers (Figure 1B). Additionally, the films of these two cellulose ethers (HM5 and H14) suggest the smallest swelling ability. The differences in the contact angle measurements seemed to influence the behaviour of these two cellulose ether films. M1 could not be evaluated. It was not possible to recognize a connection between swelling and shrinking behaviour of the different cellulose ethers dependent on their substitution type or their viscosity grade.

Conclusions

Raman spectroscopy and ESEM techniques are suitable and powerful methods to examine the interactions of excipients, such as cellulose ethers, with water. Based on the Raman spectra of cellulose ethers, a classification by their substitution types is possible, but it is not possible to distinguish the cellulose ethers by their viscosity grade. The influence of absorbed water on cellulose ether raw materials and of swollen cellulose ethers are quantified in Raman spectra. The intensity ratios of some Raman bands remain after drying the gels. The Raman studies reveal that the molecular structures of gels and films are similar. The several structurings of the cellulose ether film surfaces are visible in SEM and ESEM micrographs. Quantitative information on swelling and shrinking of cellulose ethers can be gained by in-situ ESEM experiments. For these, the surfaces have to be coated with a special pattern thin metal layer. Raman spectroscopy and ESEM are complementary methods to characterize morphological, as well as molecular, properties. The coupling of both could provide information at the same time. The interaction of cellulose ethers with water depends on their substitution type. All differences described are differences in the type of substitution.

References

Achanta, A. S., Adusumilli, P. S., James, K. W., Rhodes, C. T. (2001) Thermodynamic analysis of water interaction with excipient films. *Drug Dev. Ind. Pharm.* **27**: 227–240

Alderman, D. A. (1984) A review of cellulose ethers in hydrophilic matrices for oral controlled-release dosage forms. *Int. J. Pharm. Tech. Prod. Mfr* **5**: 1–9

Alvarez-Lorenzo, C., Lorenzo-Ferreira, R. A., Gomez-Amoza, J. L., Martinez-Pacheco, R., Souto, C., Concheiro, A. (1999) A comparison of gas-liquid chromatography, NMR spectroscopy and Raman spectroscopy for determination of the substituent content of general non-ionic cellulose ethers. *J. Pharm. Biomed. Anal.* **20**: 373–383

Alvarez-Lorenzo, C., Gomez-Amoza, J. L., Martinez-Pacheco, R., Souto, C., Concheiro, A. (2000) Interactions between hydroxypropylcelluloses and vapour/liquid water. *Eur. J. Pharm. Biopharm.* **50**: 307–318

Blackwell, J., Vasko, P. D., Koenig, J. L. (1970) Infrared and Raman spectra of the cellulose from the cell wall of Valonia ventricosa. *J. Appl. Phys.* **41**: 4375–4379

Donald, A. M. (2002) No need to dry – environmental scanning electron microscopy of hydrated system. *Mat. Res. Soc. Symp. Proc.* **711**: 93–100

Edwards, H. G. M., Farwell, D. W., Williams, A. C. (1994) FT-Raman spectrum of cotton: a polymeric biomolecular analysis. *Spectrochim. Acta* **50A**: 807–811

Edwards, H. G. M., Farwell, D. W., Webster, D. (1997) FT Raman spectroscopy of untreated natural plant fibres. *Spectrochim. Acta* **53A**: 2383–2392

Fechner, P. M., Wartewig, S., Füting, M., Heilmann, A., Neubert, R. H. H., Kleinebudde, P. (2003) Properties of microcrystalline cellulose and powder cellulose after extrusion/spheronization as studied by Fourier transform Raman spectroscopy and environmental scanning electron microscopy. *AAPS PharmSci.* **5**: Article 32

Flory, P. J. (1974) Introductory lecture. In: gels and gelling processes. *Faraday Discuss.* **57**: 7–18

Gao, P., Meury, R. H. (1996) Swelling of hydroxypropyl methylcellulose matrix tablets. 1: Characterization of swelling using a novel optical imaging method. *J. Pharm. Sci.* **85**: 725–731

Goral, J., Zichy, V. (1990) Fourier Transform Raman studies of materials and compounds of biological importance. *Spectrochim. Acta* **46A**: 253–275

Hjärtstam, J., Hjertberg, T. (1998) Swelling of pellets coated with a composite film containing ethyl cellulose and hydroxypropyl methylcellulose. *Int. J. Pharm.* **161**: 23–28

Hopfe, J., Füting, M. (1995) Fundamentals and applications of environmental scanning electron microscopy. In: Wetzig, K., Schulze, D. (eds) *In situ scanning electron microscopy in materials research*. Akademie Verlag GmbH, Berlin, pp 219–240

Jenkins, L. M., Donald, A. M. (1997) Use of the environmental scanning electron microscope for the observation of the swelling behaviour of cellulose fibres. *Scanning* **19**: 92–97

Langkilde, F. W., Svantesson, A. (1995) Identification of celluloses with Fourier-Transform (FT) mid-infrared, FT-Raman and near-infrared spectrometry. *J. Pharm. Biomed. Anal.* **13**: 409–414

Levin, I. W., Lewis, E. N. (1990) Fourier transform Raman spectroscopy of biological materials. *Anal. Chem.* **62**: 1101A–1111A

Malamataris, S., Karidas, T., Goidas, P. (1994) Effect of particle size and sorbed water on the compression behaviour of some hydroxypropyl methylcellulose (HPMC) polymers. *Int. J. Pharm.* **103**: 205–215

McCrystal, C. B., Ford, J. L., He, R., Craig, D. Q. M., Rajabi-Siahboomi, A. R. (2002) Characterisation of water behaviour in cellulose ether polymers using low frequency dielectric spectroscopy. *Int. J. Pharm.* **243**: 57–69

Mitchell, K., Ford, J. L., Armstrong, D. J., Elliott, P. N. C., Hogan, J. E., Rostron, C. (1993a) The influence of the particle size of hydroxypropylmethylcellulose K15M on its hydration and performance in matrix tablets. *Int. J. Pharm.* **100**: 175–179

Mitchell, K., Ford, J. L., Armstrong, D. J., Elliott, P. N. C., Hogan, J. E., Rostron, C. (1993b) The influence of drugs on the properties of gels and swelling characteristics of matrices containing methylcellulose or hydroxypropylmethylcellulose. *Int. J. Pharm.* **100**: 165–173

Mitchell, K., Ford, J. L., Armstrong, D. J., Elliott, P. N. C., Rostron, C., Hogan, J. E. (1993c) The influence of concentration on the release of drugs from gels and matrices containing Methocel. *Int. J. Pharm.* **100**: 155–163

Nokhodchi, A., Ford, J. L., Rowe, P. H., Rubinstein, M. H. (1996a) The influence of moisture on the consolidation properties of hydroxypropylmethylcellulose K4M (HPMC 2208). *J. Pharm. Pharmacol.* **48**: 1116–1121

Nokhodchi, A., Ford, J. L., Rowe, P. H., Rubinstein, M. H. (1996b) The effect of moisture on the Heckel and energy analysis of hydroxypropylmethylcellulose 2208 (HPMC K4M). *J. Pharm. Pharmacol.* **48**: 1122–1127

Nokhodchi, A., Ford, J. L., Rowe, P. H., Rubinstein, M. H. (1996c) The effects of compression rate and force on the compaction properties of different viscosity grades of hydroxypropylmethylcellulose 2208. *Int. J. Pharm.* **129**: 21–31

Ofner, C. M., Klech-Gelotte, C. M. (2002) Gels and jellies. In: Swarbrick, J., Boylan, J. C. (eds) *Encyclopedia of pharmaceutical technology*. Part 2, Marcel Dekker, New York, pp 1327–1344

Otto, M. (1999) *Chemometrics: statistics and computer application in analytical chemistry*. Wiley-VCH Verlag GmbH, Weinheim, p. 148

Palzer, S., Hiebl, C., Sommer, K., Lechner, H. (2001) Einfluss der Rauhigkeit einer Feststoffoberfläche auf den Kontaktwinkel. *Chemie Ing. Technik* **73**: 1032–1038

Parakh, S. R., Gothoskar, A. V., Karad, M. T. (2003) A novel method for the study of water absorption rates by swellable matrices. *Pharm. Technol.* **5**: 40–48

Rajabi-Siahboomi, A. R., Bowtell, R. W., Mansfield, P., Davies, M. C., Melia, C. D. (1996) Structure and behaviour in hydrophilic matrix sustained release dosage forms: 4. Studies of water mobility and diffusion coefficients in the gel layer of HPMC tablets using NMR imaging. *Pharm. Res.* **13**: 376–380

Rowe, R. C., Sheskey, P. J., Weller, P. J. (eds) (2003) *Handbook of pharmaceutical excipients*. 4th edn, PhP, London, Chicago, pp 289–300, 386–389

Sebti, I., Delves-Broughton, J., Coma, V. (2003) Physicochemical properties and bioactivity of nisin-containing cross-linked hydroxypropylmethylcellulose films. *J. Agric. Food Chem.* **51**: 6468–6474

Sekkal, M., Dincq, V., Legrand, P., Huvenne, J. P. (1995) Investigation of the glycosidic linkages in several oligosaccharides using FT-IR and FT Raman spectroscopies. *J. Mol. Struct.* **349**: 349–352

Siepmann, J., Kranz, H., Bodmeier, R., Peppas, N. A. (1999) HPMC-Matrices for controlled drug delivery: a new model combining diffusion, swelling, and dissolution mechanisms and predicting the release kinetics. *Pharm. Res.* **16**: 1748–1756

Stahl, P. H. (1980) *Feuchtigkeit und Trocknen in der pharmazeutischen Technologie*. Dr. Dietrich Steinkopf Verlag GmbH & Co. KG, Darmstadt, p.183

Stokes, D. J., Rea, S. M., Porter, A. E., Best, S. M., Bonfield, W. (2002) Characterisation of biomedical materials, cells and interfaces using environmental SEM (ESEM). *Mat. Res. Soc. Symp. Proc.* **711**: 113–118

Stokes, D. J., Rea, S. M., Best, S. M., Bonfield, W. (2003) Electron microscopy of mammalian cells in the absence of fixing, freezing, dehydration, or specimen coating. *Scanning* **25**: 181–184

Tai, S. S. W., Tang, X. M. (2001) Manipulating biological samples for environmental scanning electron microscopy observation. *Scanning* **23**: 267–272

Zografi, G., Johnson, B. A. (1984) Effects of surface roughness on advancing and receding contact angles. *Int. J. Pharm.* **22**: 159–176

Zografi, G., Kontny, M. J. (1986) The interactions of water with cellulose- and starch-derived pharmaceutical excipients. *Pharm. Res.* **3**: 187–194